

A Simple Global/Local Approach to Modeling Ballistic Impact onto Woven Fabrics

M. P. Rao ^a, M. Keefe ^b, B. M. Powers ^c, T. A. Bogetti ^d

^a Center for Composite Materials, University of Delaware, Newark, DE 19716

^b Department of Mechanical Engineering, University of Delaware, Newark DE 19716

^{c, d} United States Army Research Laboratory, Aberdeen Proving Ground, MD 21005

Abstract

The objective of this study is to develop and demonstrate the feasibility of an LS-DYNA[®] Global/Local model for studying the non-linear mechanics of woven fabrics under ballistic impact. The presented approach is built on the observed response of fabrics in experimental studies performed at the Army Research Laboratory (ARL). In particular, two-layer test patches of 600 denier Kevlar KM2[®] fabrics are modeled with the aim of corroborating experimentally determined V_{50} velocities and physical deformation patterns. However, the present study begins with a brief overview of detailed three-dimensional (3D) finite element models of the woven fabrics under ballistic impact, comprised of regular undulating geometries of the individual yarn. This model is designated as the Full-Local environment and serves as the baseline for the subsequent Global/Local 3D finite element models. Within this Full-Local environment, the projectile velocity is determined as a function of time, and the response of the fabrics under the applied impact load are presented and discussed. Based on this work, the Global/Local modeling framework is developed that represents the fabric finite element meshes as comprised of combinations of homogenized continuum regions ('Global' regions) which neglect yarn undulations, and full 3D undulating yarns ('Local' regions). Discussions are presented regarding the implications on the predicted ballistic response of the fabrics. Specifically, comparisons are made for the predicted projectile velocity as a function of time, fabric deformations, energy histories, and computing time required to execute the individual simulations. It is shown that the Global/Local modeling approach results in reasonable savings in computing time without appreciably sacrificing the physics of the problem.

Introduction

Woven fabrics are being actively used for ballistic protection of individuals. The flexibility accrued in the design of the protective clothing for soldiers is directly a function of the high strength/weight ratio of woven fabrics. The yarns in woven fabrics interact with the advancing projectile in a complex manner leading to the dissipation of the kinetic energy of impact. It is this interaction mechanism that is at once beneficial from an applications perspective, yet challenging to model in a computational environment.

Early studies on modeling ballistic impact [1] employed pin-jointed representations of the fabric in conjunction with spring-dashpot type models to describe the material behavior of the yarns. While these models were able to capture the material mechanics accurately, the physical problem of ballistic impact was in itself simplistic. Effects of such parameters as inter-yarn friction were inherently unaccounted for. Later models [2] based on membrane representations of the fabrics, while successfully predicted overall ballistic performance, were however, incapable to shedding light on the interaction of the individual

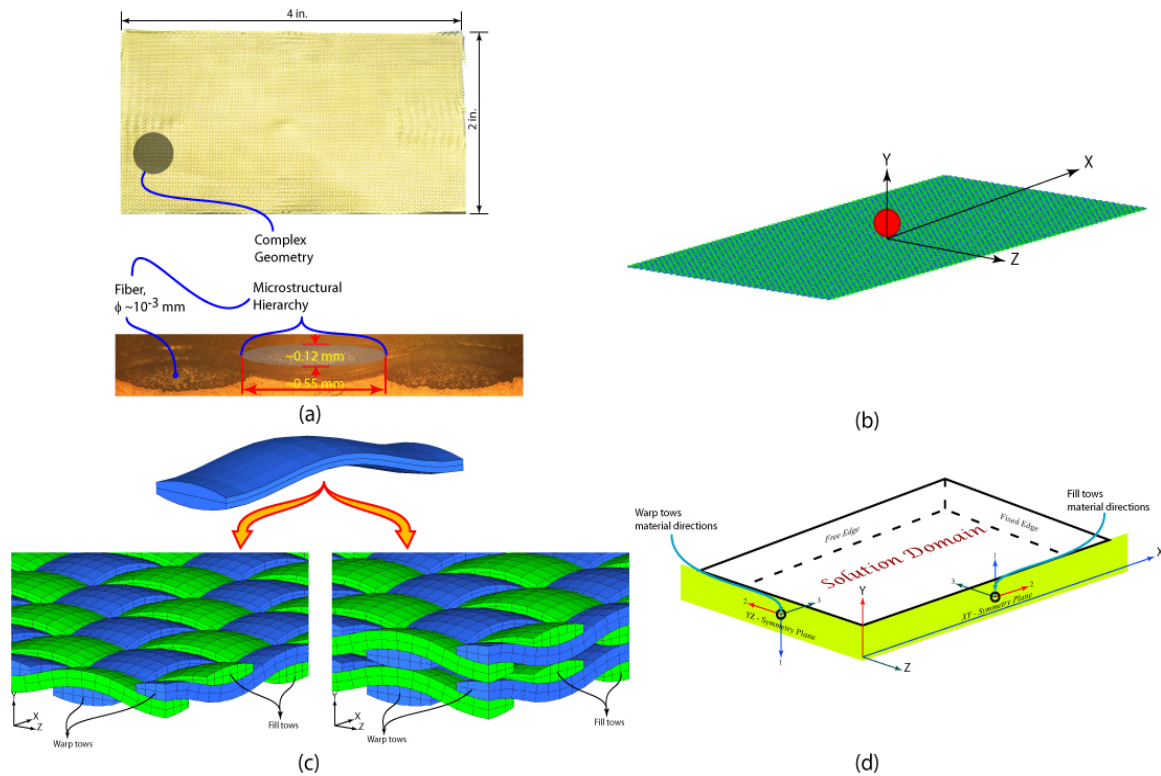


Figure 1: One- and Two-layer fabric impact system configuration. (a) Multiple length scales encompassed by the Kevlar KM2 fabric. (b) Isometric view of the projectile and one-layer fabric. (c) Details of the quarter symmetric finite element mesh. (d) Schematic of the solution domain exhibiting symmetry and edge boundary conditions along with tow principal material directions.

yarns. Tan and Ching [3] reported significant savings in computing time by modeling the fabric with bar elements, while accounting for inter-yarn friction. However these models studied only single layer fabrics of dimensions confined to those of laboratory specimens.

More recently researchers [4-8] have developed detailed three-dimensional (3D) finite element models of woven fabrics under ballistic impact. Schematically, the impact system configuration could be represented as shown in Figure 1. Two separate geometrically dissimilar modeling strategies are developed to study the problem illustrated in Figure 1. The first strategy, extensively documented in [4-8], wherein the undulating yarns are explicitly modeled in three-dimensional (3D) detail is designated as the Full-Local Solution. The second modeling technique comprises of combining 3D yarn descriptions with homogenized continuum domains that neglect undulations. This approach is termed as the Global-Local Solution [9].

Explicit Three-Dimensional Modeling of the Impact System

The plain weave fabric patch shown in Figure 1a encompasses 34 yarns per inch resulting in an areal density of 180 g/m^2 and measures 4" by 2" in planar dimensions. The impact system in Figure 1b exhibits symmetry with respect to the coordinate system shown. As such, the models in Figure 1c display the details of the FE mesh of the quarter symmetric domain of the fabric. A schematic representation of the solution domain along with tow material directions and imposed boundary conditions is presented in Figure 1d.

Consistent with previous research [4-8], the yarns in this study are modeled as transversely isotropic elastic continua, with the stiffest direction pointing along the yarn axis, invoking the *MAT_ORTHOTROPIC_ELASTIC material model. The parameter AOPT is set to 0.0. Table 1 represents the material properties of the yarns in the 1-2-3 coordinate systems shown in Figure 1d.

E ₁₁	E ₂₂	E ₃₃	G ₁₂	G ₂₃	G ₁₃	ν ₁₂	ν ₂₃	ν ₁₃
0.62	0.62	62.0	0.126	0.126	0.126	0.0	0.0	0.0

Table 1: Transversely isotropic material properties of the Kevlar KM2[®] yarns [10]. Elastic and shear moduli are reported in GPa.

Elements in which the maximum principal stress reaches 3.5 GPa [11] are deleted from the calculation with the aid of the *MAT_ADD_EROSION material model. The yarn material density is 764 Kg/m³ as reported in [9].

Contact between the projectile and fabric and between individual yarns is defined by invoking the *CONTACT_SURFACE_TO_SURFACE algorithm. Friction between the projectile and fabric is specified as $\mu_s = \mu_k = 0.18$ [8], where μ_s is the static and μ_k is the kinetic coefficient of friction, whereas between individual yarns $\mu_s = 0.23$ and $\mu_k = 0.19$ [8]. The same inter-yarn friction coefficients are also employed to specify inter-layer friction in the case of two-layer fabrics.

The projectile is modeled as a rigid sphere [12] with Hughes-Liu shell elements. The projectile diameter, $d_p = 5.35$ mm and its mass is $m_p = 0.625$ g.

By definition, V_{50} is the velocity that indicates a 50% probability of the projectile perforating the target at that velocity. Therefore the model is effective if it predicts physically reasonable behavior for either $V_s = V_{50}$ or $V_s = V_{50} \pm \sigma_{V_{50}}$, where V_s is the striking velocity, $\sigma_{V_{50}}$ is the experimentally determined standard deviation in the V_{50} data. The model is considered to have corroborated experimental V_{50} if within the above span of V_s , and duration of simulation time, the residual projectile velocity $V_r \leq 0.0$ m/s.

Explicit Modeling Results

The baseline simulation results obtained from the above detailed 3D modeling effort would be discussed in this section. These results will then be used to calibrate the performance of the Global/Local models.

Projectile Velocity

Three projectile velocities – time curves are shown in Figure 2 for the two-layer fabric impact system. The projectile velocity profile for $V_s = V_{50}$ is the green line in Figure 2 drawn along with the “□” symbols. Since $V_r = 20$ m/s at the end of simulation ($t = 250 \mu s$), two additional simulations were performed to bound and verify the LS-DYNA models. The projectile velocity profile corresponding to $V_s = V_{50} + \sigma_{V_{50}}$, is shown by the red line drawn with the “○” symbols.

As expected, this profile indicates that the projectile perforates the fabric, since the projectile is predicted to have a positive residual velocity ($V_r = 30$ m/s) at the end of simulation time. The projectile velocity profile corresponding to $V_s = V_{50} - \sigma_{V_{50}}$ is shown by the blue line drawn along with the “◇” symbols. At this striking velocity, the projectile is caught by the fabric, as indicated by $V_r = -55$ m/s at the end of simulation time. Therefore, the LS-DYNA model is considered to have successfully corroborated the experimental V_{50} data.

Physical Deformation of the Fabric

Salient snapshots of the response of the two-layer fabric are presented in Figure 3. Around $t = 110 \mu\text{s}$, the slower moving transverse wave has reached the fixed boundaries, and the projectile is free from the top layer. As a result, the yarns in the bottom layer are now responsible for absorbing bulk of the projectile’s kinetic energy. The snapshot in Figure 3b was taken at $t = 155 \mu\text{s}$, wherein the yarns in the bottom layer have completely stretched out, and the top layer has impacted the bottom layer. Although not discernible in Figure 3b, a few yarns have broken near the fixed boundaries. These yarn failure events propagate at an increasing rate beyond $t = 155 \mu\text{s}$, and as shown in Figure 3c ($t = 200 \mu\text{s}$), are also responsible for the creases in the bottom layer. Beyond $t = 200 \mu\text{s}$, the top layer is flapping free, and by the end of simulation time $t = 250 \mu\text{s}$ (see Figure 3d) is not at all in contact with the projectile. The yarns in the bottom layer are primarily responsible for slowing down the projectile beyond $t = 150 \mu\text{s}$. But their failure near the fixed boundaries renders them free of any significant constraints thereby severely impairing their ability to absorb the projectile’s kinetic energy. As such, the projectile velocity – time curves corresponding to $V_s = V_{50} + \sigma_{V_{50}}$ and $V_s = V_{50}$ plateau out as shown in Figure 2.

Global Energy History

The initial kinetic energy of the impacting projectile is computed as:

$$KE_i = \frac{1}{2} m_p V_s^2 \quad (1)$$

Temporal variations in the kinetic, internal, sliding, and hourglass energies of the two-layer woven fabric impact system are shown in Figure 4. The kinetic, internal and sliding energy curves are characterized by distinct changes in slope that correspond to particular physical events as illustrated in Figure 4. The initial kinetic energy of the system computed with the aid of Equation 1 is given by $KE_i = 8.23$ J, wherein the striking velocity is $V_s = V_{50} = 162.3$ m/s.

The decrease in kinetic energy of the system for practical purposes corresponds to the increase in internal energy until around $t = 60 \mu\text{s}$ after impact. Between $t = 60 \mu\text{s}$ and $t = 110 \mu\text{s}$, the projectile’s kinetic energy is dissipated as a combination of internal and sliding energies, although the sliding energy component increases at a much faster rate. This implies that there is significant relative motion between the yarns in the top layer, after they fail near the impact region.

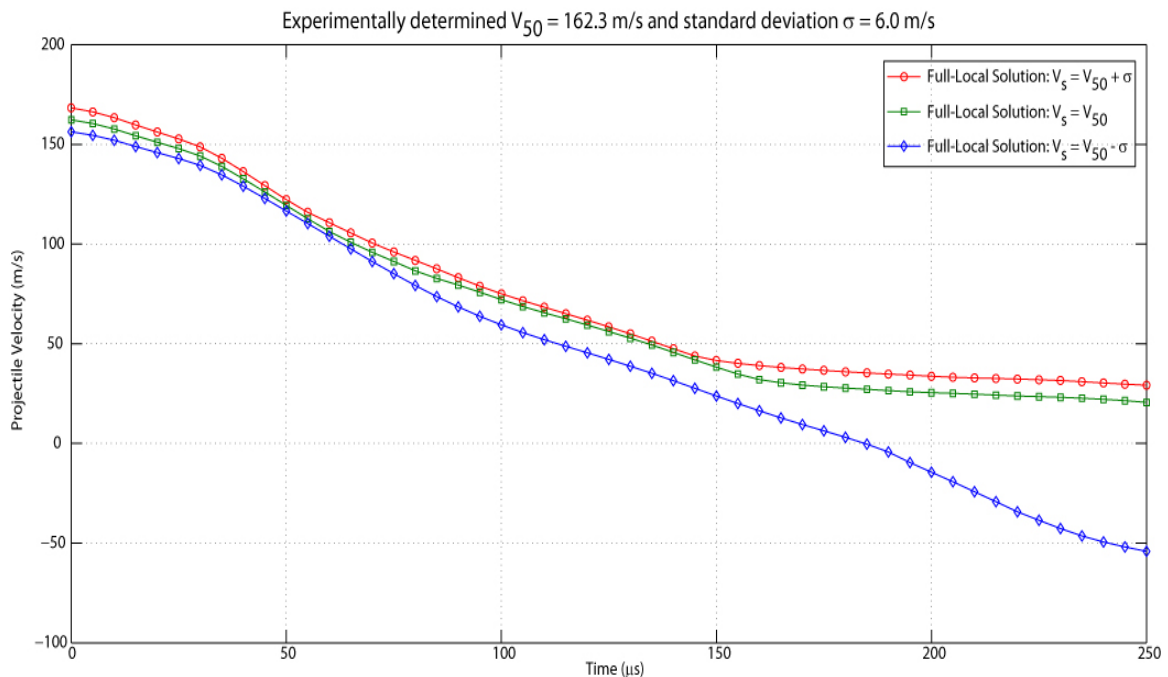


Figure 2: Predicted projectile velocity for the two-layer fabric impact system configuration.

As seen in Figure 4, between $t = 110 \mu\text{s}$ and $t = 150 \mu\text{s}$, the system internal energy peaks leading to failure of yarns in the bottom layer at the fixed edges. During the above time span, the rate of increase of sliding energy is roughly constant, indicating that predominantly, the system internal energy is responsible for dissipating the projectile's kinetic energy.

The internal energy remains practically constant, whereas the sliding energy increases sharply between $t = 155 \mu\text{s}$ and $t = 190 \mu\text{s}$, as shown in Figure 4. These consequences are associated with yarn failure in the bottom layer near the fixed edges, leading to significantly greater inter-yarn and inter-layer frictional sliding. The kinetic energy of the system begins to increase beyond $t = 195 \mu\text{s}$, that corresponds to the free flapping motion of the top layer.

Global/Local Modeling of the Impact System

Foundations

The central band of principal yarns are chiefly responsible for dissipating the projectile's kinetic energy. This assertion is supported by the results in Figure 2 and the work of Naik and Shirao [13]. The secondary yarns [13] are not appreciably involved in this process. Therefore in Figure 5, undulating 3D yarns are modeled either in a central cross pattern (Figure 5b) or central rectangular patch (Figure 5c). These domains are designated as the "Local Regions" whereas the secondary yarns [13] are replaced by homogenized continuum volumes termed as the "Global Regions." The configuration in Figure 5c is similar to the work of Barauskas and Abraitiene [14]. However in this study, only those results as applicable to the Center-Cross configuration are reported.

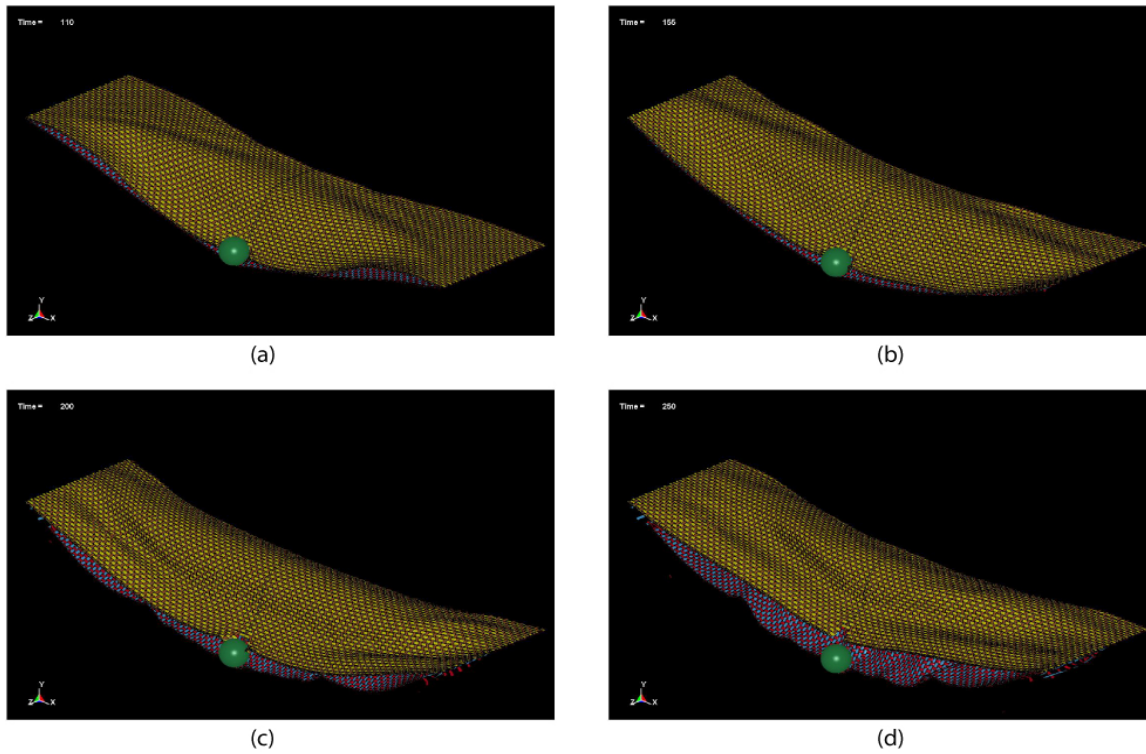


Figure 3: Predicted physical deformation of the two-layer woven fabric. (a) $t = 110 \mu s$. (b) $t = 155 \mu s$. (c) $t = 200 \mu s$. (d) $t = 250 \mu s$.

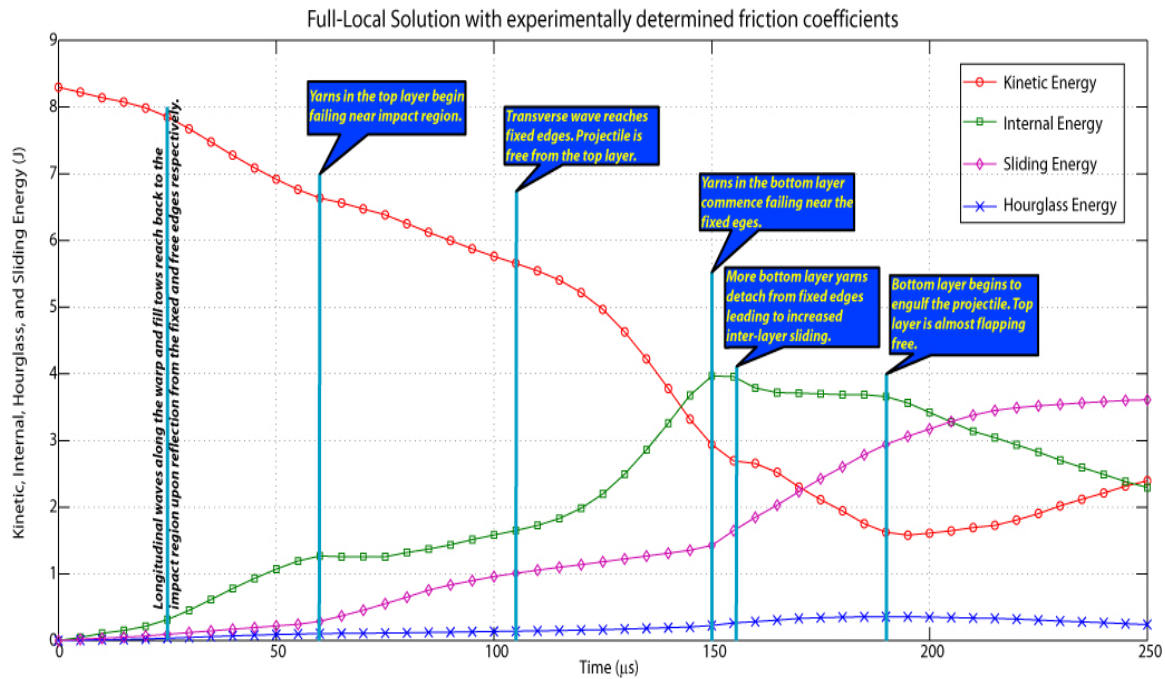


Figure 4: Global energy history for the two-layer woven fabric impact system.

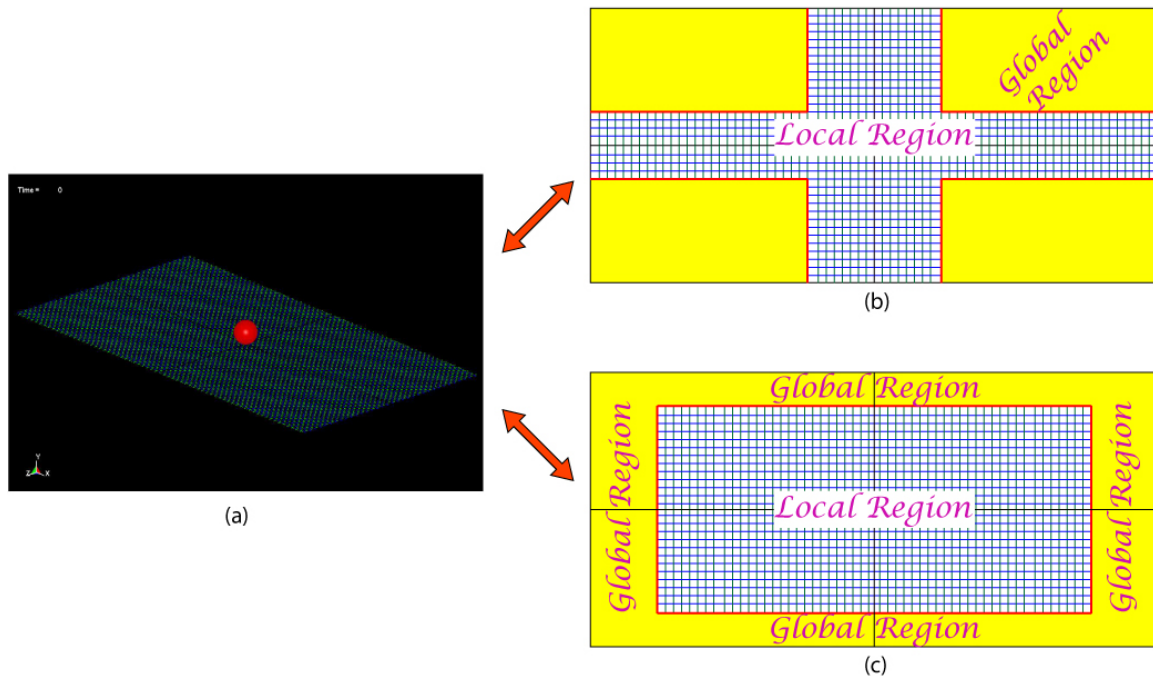


Figure 5: The concept of the Global/Local modeling approach implemented in LS-DYNA. (a) Center-Cross configuration. (c) Center-Rectangle configuration.

Nomenclature

Global/Local models are identified as α - β GL [9] wherein, ' α ' represents the mass percentage of the Global Region, and, ' β ' is the mass percentage of the Local Region, regardless of the configuration shown in Figure 5.

Geometry

At this time, there is not any *a priori* methodology available to determine the best combinations of the above mass percentages and model configurations shown in Figure 5. For the purpose of the current study, results pertaining to the 45-55GL model in the Center-Cross configuration, incorporating two-layer fabrics are reported. Detailed discussions on Global/Local modeling of one-layer fabrics are presented elsewhere [9].

Meshing

Two different meshes are developed viz., (a) solid elements for Global and Local regions – Mesh Configuration # 1, and (b) shell elements for the Global Region and solid elements for the Local Region – Mesh Configuration # 2.

In Mesh Configuration # 1, the *CONSTRAINED_LAGRANGE_IN_SOLID algorithm is employed to constrain the Global – Local interface in all three directions. Whereas the *CONTACT_TIED_SHELL_EDGE_TO_SURFACE algorithm is used to define a contact at Global – Local interface in Mesh Configuration # 2 by invoking the BEAM_OFFSET option.

Material Properties

There are mainly two properties that need to be computed for successfully executing a Global/Local solution. These are the material density ρ_v^g and the effective elastic modulus E_{xx}^g of the Global Region. The Local Region properties are the same as those used for Full-Local

solutions discussed earlier. ρ_v^g is computed by maintaining the same areal density in the Local and Global regions, whereas E_{xx}^g is computed by equating the acoustic impedance across the Global-Local interface [9]. The computed properties are reported in Table 2.

(a) Elastic and shear moduli (in GPa) along with in-plane and out-of-plane Poisson's ratios.								
E_{xx}	E_{yy}	E_{zz}	G_{xy}	G_{yz}	G_{xz}	ν_{xy}	ν_{yz}	ν_{xz}
0.5	9.2	9.2	0.05	0.05	0.05	0.0	0.0	0.0
(b) Global region volumetric density: $\rho_v^g = 764 \text{Kg} / \text{m}^3$								
(c) Maximum principal stress failure criterion: $\sigma_1 = \infty$ (No failure)								

Table 2: Material properties of the Global Region for the 45-55GL solution.

Global/Local Modeling Results

Projectile Velocity

The solution predicted by Mesh Configuration # 2 is stiffer than both the Full-Local and Mesh Configuration # 1 solutions. Yet it is bounded by the results shown in Figure 2. Investigations into the implications of the seemingly inconsistent results in Figure 6 are being actively pursued. The solution with Mesh Configuration # 1 ran only until 170 μs , reporting a “22 Error termination.”

Physical Deformation of the Fabric

Figure 7 shows the response of the two-layer fabric impact system as predicted by the three individual modeling strategies. At $t = 155 \mu\text{s}$, all the three solutions appear to be qualitatively similar, although the results of Figure 6 do not support this observation. However, one must recognize that the Global-Local solutions are approximations to the Full-Local solution which in itself is a simplification of the actual mechanistic problem. Therefore one has to quantitatively characterize and bound the Global-Local solutions in order to fully discern their purport. Such studies are currently in progress.

Global Energy History

The stiffness of the solution obtained with the Mesh Configuration # 2 is apparent in the kinetic and internal energy histories reported in Figure 8. However, qualitatively the kinetic energy history appears to be close enough to the same predicted by the Full-Local solution. The hourglass energy for the Mesh Configuration # 2 is the least since the Global region is meshed with fully-integrated shell elements. On the other hand, the sliding energy predicted by Mesh Configuration # 2 agrees very well with the Full-Local solution. While the hourglass energy predicted by the Mesh Configuration # 1 is the greatest since the Global region is meshed with

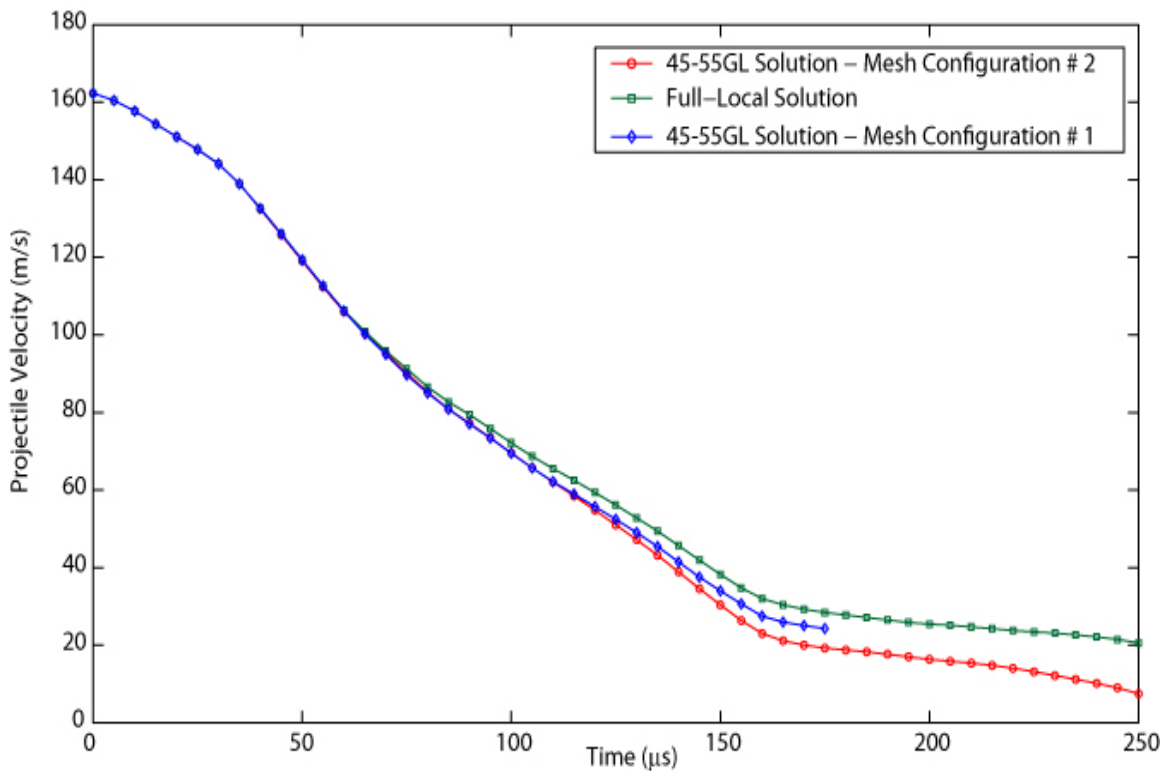


Figure 6: Comparing projectile velocity time history through the two-layer fabric impact system as predicted by the Full-Local and 45-55GL solutions.

larger reduced integration one-point quadrature solid elements, the discrepancy in predicting the sliding energy, suggests that perhaps this meshing technique is unsuitable for addressing the mechanics of the problem.

Computing Time

The time required to execute the above simulations are reported in Table 3 below:

Layers	T_{FL} (Hours)	$T_{45-55GL}^{MC1}$ (Hours)	$T_{45-55GL}^{MC2}$ (Hours)	%savings = $\left(\frac{T_{FL} - T_{45-55GL}^{MC1}}{T_{FL}}\right) \times 100$	% savings = $\left(\frac{T_{FL} - T_{45-55GL}^{MC2}}{T_{FL}}\right) \times 100$
2	19.47	NA	14.7	NA	24.5

Table 3: Computing time for individual solution strategies: $FL \Rightarrow$ Full-Local, $MC1 \Rightarrow$ Mesh Configuration # 1 and $MC2 \Rightarrow$ Mesh Configuration # 2.

Since the solution pertaining to Mesh Configuration # 1 did not run to completion, one cannot make a comparison with the Full-Local solution based on computing time. However in the case of Mesh Configuration # 2, a clear benefit is evident in pursuing a Global/Local modeling strategy based on the results in Table 3. In parallel studies it was observed that higher inter-layer friction alters the failure mechanisms resulting in significant reductions in the computing even in the Full-Local configuration. Therefore other extraneous parameters not considered herein also affect the computing time. As such, ongoing studies are aimed at addressing such issues with the objective of quantitatively bounding the Global/Local solutions.

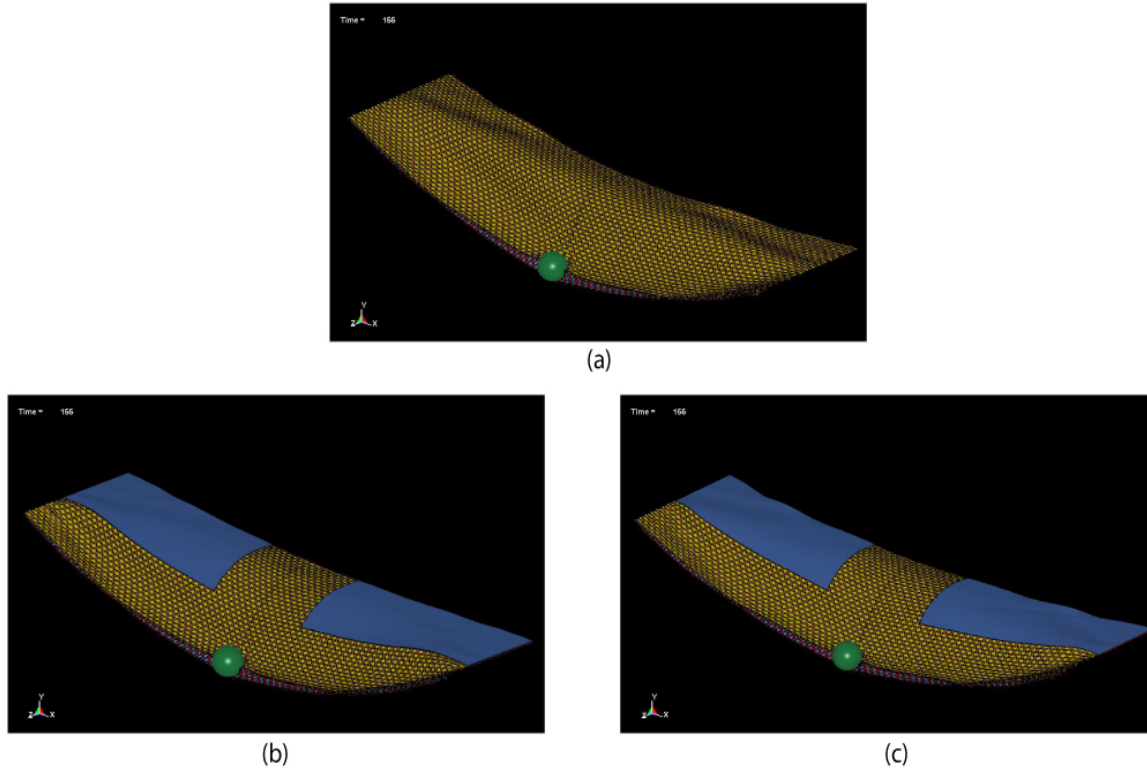


Figure 7: Back face snapshots of the two-layer fabric at $t = 155 \mu s$. (a) Full-Local Solution. (b) 45-55GL Solution – Mesh Configuration # 1. (c) 45-55GL Solution – Mesh Configuration # 2.

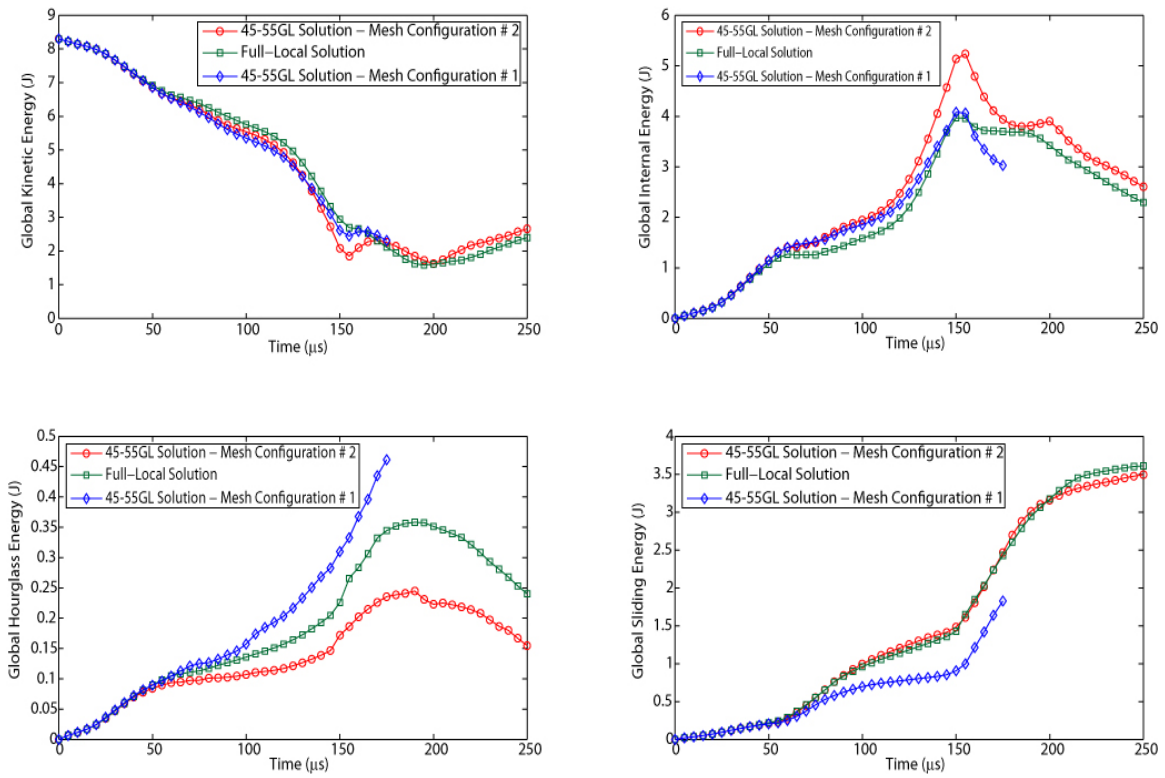


Figure 8: System energy histories for the two-layer fabric impact system as computed with the aid of the Full-Local solution and Global-Local solutions.

Conclusions

A simple yet powerful Global/Local modeling methodology has been developed for studying the impact response of woven fabric. Key aspects of the problem relating to orthotropic properties of yarns, inter-yarn, inter-layer, and projectile-fabric friction have been addressed. It was shown that while the present Global/Local models reasonably duplicate the response obtained via the Full-Local solution, there are some discrepancies that need further investigation. Chief among them is the stiffness of the Mesh Configuration # 2. As such, the reported results are the preliminary outcomes of a detailed long-term study.

References

- [1] V.P.W Shim, V.B.C. Tan and T.E. Tay 1995. "Modelling Deformation and Damage Characteristics of Woven Fabric Under Small Projectile Impact." *International Journal of Impact Engineering*, 16(4):585-608.
- [2] C.T. Lim, V.P.W. Shim and Y.H. Ng 2003. "Finite-element modeling of the ballistic impact of fabric armor." *International Journal of Impact Engineering*, 28:13-31.
- [3] V.B.C Tan and T.W. Ching 2006. "Computational simulation of fabric armour subjected to ballistic impact." *International Journal of Impact Engineering*, 32:1737-1751.
- [4] Y. Duan, M. Keefe, T.A. Bogetti and B.A. Cheeseman 2005. "Modeling the role of friction during ballistic impact of high-strength plain-weave fabric," *Composite Structures*, 68:331-337.
- [5] Y. Duan, M. Keefe, T.A. Bogetti and B.A. Cheeseman 2005. "Modeling friction effects on the ballistic behavior of a single-ply high-strength fabric," *International Journal of Impact Engineering*, 31:996-1012.
- [6] Y. Duan, M. Keefe, T.A. Bogetti and B. Powers 2006. "Finite element modeling of transverse impact on a ballistic fabric," *International Journal Mechanical Sciences*, 48:33-43.
- [7] Y. Duan, M. Keefe, T.A. Bogetti, B.A. Cheeseman and B. Powers 2006. "A Numerical investigation of the influence of friction on energy absorption by a high-strength fabric subjected to ballistic impact," *International Journal of Impact Engineering*, 32:1299-1312.
- [8] M.P. Rao, Y. Duan, M. Keefe, B.M. Powers, and T.A. Bogetti, "Studying the effects of yarn material properties and friction on the ballistic impact of a plain-weave fabric," to be submitted to *Composite Structures*.
- [9] M.P. Rao, M. Keefe, B.M. Powers, and T.A. Bogetti. Multi-scale modeling of ballistic impact onto woven fabrics. *Under review with the American Society for Composites — First submitted: December 2007 — To be included in the Special Issue of the Journal of Composite Materials featuring papers presented at the 22nd Annual Technical Conference of the American Society for Composites, Seattle, WA, September, 2007.*
- [10] H.H. Yang 2000. *Aramid fibers. Compressive Composite Materials, Fiber Reinforcements and General Theory of Composites*, 1:199 – 299, Elsevier Science, Oxford, UK.
- [11] Ming Cheng, Weinong Chen and Tuist Weerasooriya 2005. "Mechanical Properties of Kevlar[®] KM2 Single Fiber." *Journal of Engineering Materials and Technology*, 127:197-203.
- [12] Benjamin A. Schiffman and Eric D. Wetzel 2006. "Low velocity ballistic characterization of high performance fabrics." Unpublished Report. U.S. Army Research Laboratory, Aberdeen Proving Ground, MD.
- [13] N.K. Naik and P. Shrirao 2004. "Composite structures under ballistic impact." *Composite Structures*, 66:579-590.
- [14] Rimantas Barauskas and Ausra Abraitienė 2007. "Computational analysis of impact of a bullet against the multilayer fabrics in LS-DYNA." *International Journal of Impact Engineering*, 34:1286-1305.

